Published in final edited form as:
J Immunol. 2009 July 15; 183(2): 1301–1312. doi:10.4049/jimmunol.0803567.

Autocrine IL-10 induces hallmarks of alternative activation in macrophages and suppresses anti-tuberculosis effector mechanisms without compromising T cell immunity[1]

Tanja Schreiber[*,2], **Stefan Ehlers**[†,‡], **Lisa Heitmann**[*], **Alexandra Rausch**[*,2], **Jörg Mages**[§], **Peter J. Murray**[¶], **Roland Lang**[§,‖], and **Christoph Hölscher**[*]

[*]Infection Immunology, Research Center Borstel, Germany

[†]Microbial Inflammation Research, Research Center Borstel, Germany

[‡]Molecular Inflammation Medicine, Christian-Albrechts-University, Kiel, Germany

[§]Institute of Medical Microbiology, Immunology and Hygiene, Technical University Munich, Munich, Germany

[¶]Department of Infectious Diseases and Immunology, St. Jude Children's Research Hospital, Memphis, TN USA

[‖]Institute of Clinical Microbiology, University Hospital Erlangen

Abstract

Elevated IL-10 has been implicated in reactivation tuberculosis (TB). Since macrophages rather than T cells were reported to be the major source of IL-10 in TB, we analyzed the consequences of a macrophage-specific overexpression of IL-10 in transgenic mice (macIL-10-transgenic) after aerosol infection with *Mycobacterium tuberculosis* (*Mtb*). MacIL-10-transgenic mice were more susceptible to chronic *Mtb* infection than non-transgenic littermates, exhibiting higher bacterial loads in the lung after 12 weeks of infection and dying significantly earlier than controls. The differentiation, recruitment and activation of TH1 cells as well as the induction of IFN-gamma-dependent effector genes against *Mtb* were not affected by macrophage-derived IL-10. However, microarray analysis of pulmonary gene expression revealed patterns characteristic of alternative macrophage activation that were overrepresented in *Mtb*-infected macIL-10-transgenic mice. Importantly, arginase-1 gene expression and activity were strikingly enhanced in transgenic mice accompanied by a reduced production of reactive nitrogen intermediates. Moreover, IL-10-dependent arginase-1 induction diminished anti-mycobacterial effector mechanisms in macrophages. Together, macrophage-derived IL-10 triggers aspects of alternative macrophage activation and promotes *Mtb* recrudescence independent of overt effects on anti-TB T cell immunity.

Keywords

bacterial infection; cytokines; monocytes/macrophages; rodent

[1]Supported by a research grant (“Host defence against infections”) from the Medical University of Lübeck to C.H., BMBF grants NIES05T22 to S.E., 01KI0784 to S.E. and C.H., and NGFN-2 FKZ 01GS0402 to R.L., the Deutsche Forschungsgemeinschaft La 1262/3−1 to R.L., and NIH grant AI062921 to P.J.M..

3Address correspondence to Christoph Hölscher, Infection Immunology, Research Center Borstel, Parkallee 22, D-23845 Borstel, Germany. Phone: ++49−4537−188−586; Fax: ++49−4537−188−775; E-mail: choelscher@fz-borstel.de.
[2]Present addresses: T.S., Center for Biological Safety, Robert Koch-Institute, Berlin, Germany; A.R., GDD Common Mechanism Research, Bayer Schering Pharma AG, Berlin, Germany.

Introduction

Tuberculosis (TB) is one of the most prevalent bacterial infections world-wide and constitutes a leading global health threat (1). Human TB caused by *Mycobacterium tuberculosis* (*Mtb*) is responsible for 8 million new cases and nearly 2 million deaths annually. Primary TB is thought to depend on a combination of genetic susceptibility of the host and virulence of the infecting *Mtb* strain, whereas post-primary TB is due to a temporal dysregulation of otherwise intact immune defenses. More detailed elucidation of the balance between protective and inflammatory immune responses to *Mtb* may accelerate the development of more effective vaccines and therapies targeting both or either form of TB.

The cell-mediated immune response is known to be critical in the host defence against infection with intracellular pathogens such as mycobacteria. T helper 1 (TH1) lymphocytes play an important role in granuloma formation by secreting type 1 cytokines, primarily interferon-gamma (IFNγ) and tumour-necrosis-factor (TNF) (2,3). These cytokines stimulate the anti-microbial activity of infected macrophages, allowing intracellular bacterial killing through reactive nitrogen intermediates (RNI) and LRG-47 (4,5). Interleukin (IL)-12 indirectly promotes an effective cell-mediated immune response by inducing IFNγ production from T and NK cells. On the other hand, these protective T cell-mediated immune responses also play a causative role in the development of the pathology of this type of chronic disease (6). Hence, down-regulation of the inflammatory response by endogenous factors that limit tissue damage, can promote establishment of chronic infection and may also lead to reactivating TB. In fact, increased levels of TH2-type anti-inflammatory cytokines such as IL-4 and IL-10 were detected in patients suffering from post-primary disease (7).

IL-10 is produced by macrophages, T cells, B cells, and a variety of other cell types. The effects of IL-10 on immune responses are mostly inhibitory (8). In macrophages, IL-10 inhibits anti-microbial effector mechansims, the expression of co-stimulatory molecules and the production of proinflammatory cytokines (9,10). Inhibition of IL-12 production by IL-10 (11) may be one mechanism by which IL-10 blocks the development of protective TH1 immune responses (12). The absence of IL-10 causes overproduction of inflammatory cytokines (13) and the development of chronic inflammatory bowel disease (14). On the other hand, IL-10-deficient ($^{-/-}$) mice also show increased resistance to intracellular pathogens such as *Listeria monocytogenes* (15), *Leishmania major* (16), and *Trypanosoma cruzi* (17). Therefore, IL-10 is required to prevent immunopathology, but it can also impair protective responses against several pathogens. The immunoregulatory function of IL-10 and the fact that elevated levels of IL-10 have been detected in TB patients (18,19) suggest a role for IL-10 in susceptibility to TB. However, one report of *Mtb* infection in IL-10$^{-/-}$ mice found neither increased protective immune responses nor in exacerbated immunopathology (20).

By contrast, mice lacking IL-10 were shown to clear *M. bovis* BCG infection more efficiently (21). Taken together, further investigation of *Mtb* infection in different IL-10 genetic models differing in the level or source of IL-10 production appear warranted. Indeed, mice overexpressing IL-10 in activated T cells (tIL-10^{tg} mice) were previously reported to be more susceptible to *Mtb* infection, exhibiting an impaired TH1 development as characterized by decreased numbers of activated T cells in the blood circulation and lung tissue (22). Similarly, another T cell specific IL-10 transgenic model was also shown to have an increased *M. bovis* BCG burden (23). However, because IL-10 is only overexpressed in these mice when T cells become activated, effects of overproduction of IL-10 by innate immune cells could not be studied.

We were interested in analyzing the consequences of a macrophage-specific overexpression of IL-10 during experimental TB for the following reasons: first, macrophages rather than T

cells were reported to be the major source of IL-10 in TB patients (18) and second, reactivation disease in patients is typically associated with a strong, rather than diminished, TH1 immune response (24). In this study, infection of mice expressing an epitope-tagged IL-10 under control of the human CD68 promoter specifically in macrophages (macIL-10^{tg} mice) (25) resulted in a very different immunological phenotype than reported for *Mtb*-infected tIL-10^{tg} mice. Even though macIL-10^{tg} mice were also more susceptible to *Mtb* infection than non-transgenic littermates, the differentiation, recruitment and activation of TH1 cells as well as the induction of IFNγ-dependent effector genes against *Mtb* were unaffected by macrophage-derived IL-10. Transcriptome analysis revealed that after *Mtb* infection genes preferentially expressed in macrophages were specifically modulated in the lungs of macIL-10^{tg} mice. Among these, genes typical for alternative macrophage activation, such as *Arg1*, were significantly induced in the lung transcriptome of *Mtb*-infected macIL-10^{tg} mice. Together, our study revealed that macrophage-derived IL-10 induces alternatively activated macrophages and promotes exacerbation of chronic *Mtb* infection in the face of intact T cell immunity.

Materials and Methods

Mice and macrophages

Transgenic mice (macIL-10^{tg} mice) specifically expressing IL-10 in macrophages under control of the human CD68 promoter were bred under specific-pathogen-free conditions at the Technical University of Munich (25). macIL-10^{tg} mice were on a FVB genetic background and transgene-negative littermates were used as controls (FVB). Myeolid-specific arginase-1-deficient $Tie2^{cre}$ Arg-$1^{flox/flox}$ mice were housed at St. Jude Children's Research Hospital (26). In any given experiment, mice were matched for age and sex. For experiments, mice were maintained under barrier conditions in the BSL 3 facility at the Research Center Borstel in individually ventilated cages. All experiments performed were in accordance with the German Animal Protection Law and were approved by the Animal Research Ethics Board of the Ministry of Environment, Kiel, Germany.

Bone-marrow-derived macrophages (BMM) were obtained after flushing of femora from $Tie2^{cre}$-pos Arg-$1^{flox/flox}$ mice and cre-negative littermates. To generate BMM, bone marrow cells were cultivated in L-929 conditioned medium as source for M-CSF activity for 9 days (27).

Bacteria and infection

Mtb (H37Rv) and *M. avium* (TMC724; originally obtained from Dr. F. Collins, Trudeau Institute, Saranac Lake, NY) were grown in Middlebrook 7H9 broth (Difco, Detroit, MI) supplemented with Middlebrook OADC enrichment medium (Life Technologies, Gaithersburg, MI), 0.002 % glycerol, and 0.05 % Tween 80. Midlog phase cultures were harvested, aliquoted, and frozen at −80°C. After thawing, viable cell counts were determined by plating serial dilutions of the cultures on Middlebrook 7H10 agar plates followed by incubation at 37°C. All experiments were performed in the BSL 3 laboratories at the Research Center Borstel. Before infection of experimental animals, stock solutions of mycobacteria were diluted in sterile distilled water and pulmonary infection was performed using an inhalation exposure system (Glas-Col, Terre-Haute, IN). To infect mice with 100 CFU *Mtb* or 10^5 *M. avium* per lung, animals were exposed for 40 min to an aerosol generated by nebulizing approximately 5.5 ml of a suspension containing 2×10^5 or 1×10^9 live bacteria per ml, respectively. Inoculum size was checked 24 h after infection by determining the bacterial load in the lung of infected mice. Mice were regularly weighed before and after infection. In accordance with the Animal Research Ethics Board of the Ministry of Environment, mice that lost 25% of their original weight during the course of infection had to be sacrificed.

Colony enumeration assays

Bacterial loads in lung, liver and spleen were evaluated at different time points after infection with mycobacteria to follow the course of infection. Organs from sacrificed animals were removed aseptically, weighed and homogenised in PBS containing a proteinase inhibitor cocktail (Roche Diagnostics, Mannheim, Germany) for subsequent quantification of cytokines prepared according to the manufacturer's instructions. Tenfold serial dilutions of organ homogenates were plated in duplicates onto Middlebrook 7H10 agar plates containing 10 % OADC and incubated at 37°C for 19−21 days. Colonies on plates were enumerated and results expressed as $\log_{10}$ CFU per organ.

Immunohistology

One lung lobe per mouse was fixed in 4% formalin-PBS, set in paraffin blocks, and sectioned (2−3 μm). For immunohistological detection of NOS2, tissue sections were deparaffinized, placed in 10 mm sodium citrate buffer (pH 6·0) and then pressure-cooked for exactly 1 min. After blocking for 20 min in 1% H_2O_2 solution, slides were incubated with appropriately diluted polyclonal rabbit anti-mouse inducible nitric oxide synthase (NOS2) (Biomol, Hamburg, Germany) in Tris-buffered saline (TBS) /10% fetal calf serum (FCS), for 30 min in a humid chamber. Appropriately diluted goat anti-rabbit immunoglobulin G (IgG) (bridging antibody) (Dianova, Hamburg, Germany) and diluted rabbit anti-goat IgG-peroxidase conjugate (tertiary antibody) (Dianova) were used in sequential incubations of 30 min each. For immunohistological detection of B cells, deparaffinized sections were blocked in H_2O_2 and sequentially incubated with a monoclonal rat anti-mouse CD45R / B220 antibody appropriately diluted in 10 % FCS / PBS, a biotinylated goat anti-rat antibody and streptavidin-horse radish peroxidase (all from BD Bioscience, Heidelberg, Germany). Development was performed using 3,3-diaminobenzidine (Sigma, Deisenhofen, Germany) and urea superoxide (Sigma), and hemalum was used to counterstain the slides.

RNA isolation and microarray analysis of pulmonary gene expression

Before and at different time points after aerosol infection with *Mtb*, weighed lung samples were homogenized in 5 ml of 4 M guanidinium-isothiocyanate buffer and total RNA was extracted by acid phenol extraction.

Affymetrix GeneChips were used for genome-wide expression analysis of the impact of IL-10 overexpression during pulmonary *Mtb* infection. Tissue from individual mice was processed as biological duplicates (untreated controls and day 25 after infection) and triplicates (day 42 after infection). Per sample, 3 μg total lung RNA was processed using the GeneChip Expression 3’ Amplification One-Cycle Target Labeling Kit according to the manufacterer's instruction. Biotinylated cRNA was hybridized on MOE430A 2.0 GeneChips, that were stained, washed and scanned following standard procedures. Microarray data were deposited in the Gene Expression Omnibus database, the accession number will be made available before publication of the paper. CEL files were processed for global normalization and generation of expression values using the robust multi-array average algorithm (RMA) in the R affy package (http://www.R-project.org). To identify differentially regulated genes, a combination of filtering for absolute (max-min > 50) and relative (max/min > 2) change across all conditions, and statistical testing using ANOVA for the variables “infection” and “genotype” was applied. Correction for multiple testing was done using Benjamini-Hochberg (28). The 4188 probe sets passing the filtering criteria were then subjected to hierarchical clustering and visualization procedures using the Spotfire DecisionSite Functional Genomics software. Data mining of differentially regulated gene lists for enrichment of co-citations with cells and tissues was performed using Genomatix Bibliosphere software (Genomatix, Germany).

RT-PCR

From extracted RNA, cDNA was obtained using murine moloney leukemia virus (MMLV) reverse transcriptase (Invitrogen, Karlsruhe, Germany) and oligo-dT (12−18mer; Sigma) as a primer. Quantitative PCR was performed on a Light Cycler (Roche Diagnostics Corporation, Indianapolis, IN) as previously described (36). Data were analyzed employing the "Fit Points" and "Standard Curve Method" using *hprt* as housekeeping gene to calculate the level of gene expression normalized for *hprt* expression. The following primer sets were employed: *Hprt*: sense 5'-GCA GTA CAG CCC CAA AAT GG-3', antisense 5'-AAC AAA GTC TGG CCT GTA TCC AA-3'; *Tnf*: sense 5'-TCT CAT CAG TTC TAT GGC CC-3', antisense 5'-GGG AGT AGA CAA GGT ACA AC-3', *IL-12p40* (*Il12b*): sense 5'-CTG GCC AGT ACA CCT GCC AC-3', antisense 5'-GTG CTT CCA ACG CCA GTT CA-3', *Nos2*: sense 5'-AGC TCC TCC CAG GAC CAC AC-3', antisense 5'-ACG CTG AGT ACC TCA TTG GC-3', *LRG-47* (*Irgm1*): sense 5'-AGC CGC GAA GAC AAT AAC TG-3', antisense 5'-CAT TTC CGA TAA GGC TTG G-3', *Arg1*: sense 5'-CAG AAG AAT GGA AGA GTC AG-3', antisense 5'-CAG ATA TGC AGG GAG TCA CC-3', *Mmr*: sense 5'-CCA CAG CAT TGA GGA GTT TG-3', antisense 5'-ACA GCT CAT CAT TTG GCT CA-3', *Ym1*: sense 5'-GGG CAT ACC TTT ATC CTG AG-3', antisense 5'-CCA CTG AAG TCA TCC ATG TC-3', *Fizz*: sense 5'-TCC CAG TGA ATA CTG ATG AGA-3', antisense 5'-CCA CTC TGG ATC TCC CAA GA-3', *Il4ra*: sense 5'-TGT GAC CTA CAA GGA ACC CA-3', antisense 5'-GCA AAA CAA CGG GAT GCA GA-3'.

Preparation of single cell suspensions

Antigen-specific restimulation and flowcytometric analysis, single cell suspensions of mediastinal lymph nodes and lungs were prepared from *Mtb*-infected mice at different time points. Lymph node cells were isolated by straining through a metal sieve. After depletion of erythrocytes, cells were resuspended in complete Iscoves-modified Dulbeccos medium (IMDM; Invitrogen) supplemented with 10 % FCS (Gibco), 0.05 mM β-mercaptoethanol (Sigma, Deisenhofen, Germany), and penicillin and streptomycin (100 U/ml and 100 μg/ml; Invitrogen), counted and used for further experiments. For preparation of single cell suspensions from lungs, mice were anesthetized and injected intraperitoneally with 150 U Heparin (Ratiopharm, Ulm, Germany). Lungs were perfused through the right ventricle with warm PBS. Once lungs appeared white, they were removed and sectioned. Dissected lung tissue was then incubated in collagenase A (0.7 mg/ml; Roche Diagnostics, Mannheim, Germany) and DNase (30 μg/ml; Sigma) at 37°C for 2 h. Digested lung tissue was gently disrupted by subsequent passage through a 100 μm pore size nylon cell strainer. Recovered lung cells were counted, diluted in IMDM and used for further experiments.

Flowcytometric analysis of surface markers and intracellular cytokines

For flowcytometric analysis of surface markers, cells were washed and incubated with a cocktail containing anti-FcγRIII/II mAb (clone 2.4G2), mouse and rat serum to block non-specific binding to Fc receptors. Cells were then incubated in consecutive steps for 20 min with optimal concentrations of the following antibodies, CD4-APC, CD3-PerCP, CD44-FITC, CD62L-PE, IA^q-PE, CD124-PE (IL-4Rα) (all from BD Biosciences) and F4/80-AlexaFluor647 (Caltag; Invitrogen), CD206 (MMR)(Serotec, Düsseldorf, Germany). For detection of intracellular IFNγ, an intracellular cytokine staining kit was employed (BD Biosciences). Briefly, single cell suspensions were prepared at 19 days after infection and 2×10^6 cells were stimulated with plate-bound anti-CD3/CD28 mAb (clone 2C11 and clone 37/51 at 10 μg/ml, respectively) for 4 h in the presence of GolgiPlug™ (BD Biosciences). Non-specific antibody binding was blocked by incubation with a cocktail containing anti-FcγRIII/II mAb (clone 2.4G2), mouse and rat serum. Cells were washed and incubated with optimal concentrations of anti-CD4-FITC (BD Biosciences). After staining, cells were fixed and

permeabilized with Cytofix/Cytoperm™ (BD Biosciences) and intracellularly accumulated IFNγ was stained with a PE-labelled anti-IFNγ mAb (BD Biosciences).

Fluorescence intensity was analysed on a FACSCalibur (BD Biosciences) gating on propidiumiodide-negative macrophages orr lymphocytes identified by FSC-SSC-profile, respectively.

IL-10 release and antigen-specific restimulation of $CD4^+$ T cells

To detect IL-10 release in lymph nodes and lungs, 3×10^6 cells from single cell suspensions of mediastinal lymph nodes and perfused lungs were cultured for 24 h in complete RPMI 1640 (Gibco) supplemented with 10 % FCS (Gibco), 0.05 mM β-mercaptoethanol (Sigma), and penicillin and streptomycin (100 U/ml and 100 μg/ml; Gibco). Supernatants were collected and frozen at −80°C until production of IL-10 was quantified by ELISA. For measuring antigen-specific production of IFNγ by $CD4^+$ T cells in lymph nodes, single cell suspension of mediastinal lymph nodes were prepared in IMDM from mice 19 days after infection with *Mtb*. To enrich $CD4^+$ T cells, single cell suspensions from lymph nodes were incubated with magnetic CD4 microbeads (Miltenyi, Bergisch Gladbach, Germany) and separated from other cells on a MACS separation unit (Miltenyi). Separated $CD4^+$ T cells were collected in IMDM, counted and diluted. Purity of enriched $CD4^+$ T cells was >95 % as determined by flow cytometry. For antigen-specific restimulation, 4×10^5 enriched $CD4^+$ lymph node cells were incubated with 2×10^5 peritoneal macrophages that were pulsed with 25 μg/ml short-term culture filtrate (ST-CF) from *Mtb* (a kind gift of Peter Andersen, Copenhagen, Denmark) in IMDM. Resident peritoneal macrophages were obtained one day prior to the experiment by peritoneal lavage of uninfected C57BL/6 mice and incubated overnight in 96 well flat-bottom microplates (Nunc, Naperville, IL) in complete IMDM. After 72 h of restimulation, supernatants were collected and frozen at −80°C until production of IFNγ was quantified by ELISA.

Quantification of IFN-γ and IL-10 by ELISA

To determine cytokine production after pulmonary infection of experimental animals, supernatants were analysed in 3-fold serial dilutions using the sandwich ELISA system OptEia™ (BD Biosciences). After incubation with horseradish peroxidase coupled to avidin and developing with TMB substrate reagent, the absorbance was read on a microplate reader (Sunrise; Tecan, Männedorf, Switzerland). Using a test wavelength of 450nm and a reference wavelength of 630nm samples, were compared to appropriate recombinant cytokine standards. The detection limits for all cytokines were 5 pg/ml.

Arginase activity in BMMφ and lung homogenates

To determine arginase activity in murine tissue, weighed pieces of organs were homogenized in 100 μl of 0.1 % Triton X-100 (Sigma) containing a protease inhibitor cocktail (Roche). 50 μl of 10 mM $MnCl_2$ (Merck), 50 mM Tris-HCl (Merck) were added to all samples and the enzyme was activated by heating for 10 min at 55°C. Arginine hydrolysis was conducted by incubating 25 μl of the activated lysate with 25 μl of 0.5 M L-arginine (Merck) at 37°C for 60 min. The reaction was stopped with 400 μl of H_2SO_4 (96%) / H_3PO_4 (85%) / H_2O (1/3/7, v/v/v). As a degree of arginase activity, the urea concentration was measured at 540 nm after addition of 25 μl α-isonitrosopropiophenone (Sigma; dissolved in 100% ethanol) followed by heating at 95°C for 45 min. One unit of arginase activity is defined as the amount of enzyme that catalyzes the formation of 1 μmol urea/min.

Detection of RNI

To detect RNI in uninfected and infected mice, blood was collected at different time points. Utilizing a commercial nitrate reductase kit (Cayman; Axxora, Lörrach, Germany) NO_3 was converted into NO_2. After adding Griess reagents, the content of NO_2 was determined by photometric measurement reading the absorbance at 540 nm on a microplate reader (Sunrise; Tecan) as previously described (27).

IFN-©-induced bacterial growth inhibition in macrophages

To analyse the anti-bacterial activity of macrophages, BMM\ were cultured 48 h before infection with *Mtb* in DMEM supplemented with 10 % FCS (Biochrom, Berlin, Germany), 2 mM L-glutamine, 1 mM sodium pyruvate, 10 mM HEPES (all from PAA, Cölbe, Germany) in the presence of medium, or incubated with 10 ng/ml IL-4 (BD Bioscience) and 10 ng/ml IL-10 (BD Bioscience). One day before infection, cells were incubated with medium or stimulated with 100 U/ml IFN-© (Peprotech, Hamburg, Germany). Cells were inoculated with *Mtb* H37Rv at a MOI of 0.5 for 2 h. To determine bacterial uptake at different time points, macrophages were lysed by addition of 0.5 % Triton X100 (Serva, Heidelberg, Germany). Lysates were serially diluted in 0,05 % Tween 80 (Merck), plated on Middlebook 7H10 agar containing 10 % OADC and incubated at 37°C for 19−21 days. Colonies on plates were enumerated and results expressed as $\log_{10}$ CFU per culture.

Statistical analysis

Quantifiable data are expressed as the means of individual determinations and standard deviations. Statistical analysis was performed using the unpaired Student's *t* test defining different error probabilities (*, $p \leq 0.05$; **, $p \leq 0.01$; ***, $p \leq 0.001$). ANOVA was performed using the Dunnett Multiple Comparison test, correcting for multiple testing, that defines different error probabilities between untreated cells and macrophages that have been incubated with IFNγ (#, $p \leq 0.05$; ##, $p \leq 0.01$) or IL-4/IL-10/IFNγ (*, $p \leq 0.05$; **, $p \leq 0.01$) , correcting for multiple testing.

Results

macIL-10tg mice are highly susceptible to Mtb infection

To determine the influence of increased levels of macrophage-derived IL-10 on the outcome of experimental TB, mice overexpressing IL-10 under control of the macrophage-specific CD68 promoter were infected with 100 CFU of *Mtb* via the aerosol route. Whereas FVB control mice were able to control mycobacterial growth in infected lungs at a plateau level of approx. 6.9 $\log_{10}$ CFU/lung, bacterial loads in IL-10-transgenic littermates steadily increased reaching significantly higher CFU counts 78 days post-infection (Fig. 1a). *Mtb*-infected FVB wildtype mice survived for more than 250 days (Fig. 1b). In contrast, macIL-10^{tg} animals died significantly earlier, with a mean survival time of approx. 100 days.

Activation of $CD4^+$ T cells is not impaired in Mtb-infected macIL-10^{tg} mice

Priming in lymphoid organs and migration of T lymphocytes to the site of infection is indispensable for the induction of defense-mechanisms against *Mtb*. In order to evaluate whether T cell activation in macIL-10^{tg} mice was impaired in draining lymph nodes and lung tissue, activated $CD4^+$ T cells were quantified by flow cytometry. After infection with *Mtb*, comparably increasing relative and absolute numbers of activated $CD44^{high}CD62L^{low}$ $CD4^+$ T cells were observed in lymph nodes of both FVB and macIL-10^{tg} mice (Fig. 2a and b). Antigen-specific restimulation of $CD4^+$ T cells purified from the draining lymph nodes revealed that T cells of macIL-10^{tg} mice were as capable of producing IFNγ as wildtype littermates (Fig. 2c). In addition, the relative proportion of activated $CD44^{high}CD62L^{low}$

$CD4^+$ T cells in the lung was also not affected during the course of *Mtb* infection in macIL-10^{tg} mice (Fig. 2d). However, the absolute amount of activated $CD4^+$ T cells in lungs from macIL-10^{tg} mice was found to be enhanced at day 84 after *Mtb* infection (Fig. 2e). After polyclonal restimulation, IFNγ-production by $CD4^+$ T cells was comparable in *Mtb*-infected FVB and macIL-10^{tg} mice (Fig. 2d). Together, macrophage-derived IL-10 did not dramatically affect the induction, migration and function of T effector cells after *Mtb* infection. The increased infiltration of activated $CD4^+$ T cells into lungs from macIL-10^{tg} mice may reflect an increased inflammatory reaction to the elevated bacterial load at late time points of *Mtb* infection.

The expression of NOS2 and LRG-47 (Irgm1) is not impaired in macIL-10tg mice after Mtb-infection

IFNγ-dependent activation of macrophages at the site of infection is key to the induction of the effector molecules NOS2 and LRG-47 (4,5) and IL-10 has been previously described to affect anti-microbial effector mechanisms (29,30). Since the expression of T cell-derived IFNγ was not affected in *Mtb*-infected macIL-10^{tg} mice, downstream effector mechanisms could have been directly impaired by the macrophage-specific overexpression of IL-10. Quantitative real time PCR revealed that during *Mtb* infection transcripts for *Nos2* were increasingly induced in lungs from both FVB and macIL-10^{tg} mice to the same extent (Fig. 3a). In fact, at day 90 post-infection, *Nos2* gene expression was found to be even higher in transgenic animals. It should be noted that IL-10 has been shown to induce *Nos2* expression in some settings suggesting that *Nos2* is not a canonical target of the IL-10 anti-inflammatory response (31). The kinetics of gene expression of *Lrg-47* (*Irgm1*) was comparable in the lungs of both FVB and macIL-10^{tg} mice peaking on day 21 of *Mtb* infection (Fig 3b). Six weeks after infection, immunohistochemical detection of NOS2 in lung sections verified these findings on the protein level showing no differences in NOS2-expression between FVB and macIL-10^{tg} mice (Fig. 3c).

Macrophage-derived IL-10 specifically suppresses IL-12p40 in infected tissue but not in draining lymph nodes

So far, the increased susceptibility of macIL-10^{tg} mice to experimental TB could neither be attributed to an impaired function of IFNγ-producing T cells nor to defective IFNγ-dependent downstream mechanisms in macrophages. IL-10 specifically suppresses the production of pro-inflammatory cytokines in activated macrophages and dendritic cells (9,32). To evaluate the suppressive effect of macrophage-derived IL-10 on anti-TB effector cytokines during the course of infection with *Mtb*, we compared the expression of TNF (produced by T cells and macrophages/dendritic cells) and IL-12p40 (produced by macrophages/dendritic cells) in the lungs of FVB wildtype and IL-10^{tg} mice. Until day 90 after infection, increasing amounts of *Tnf* transcripts were found in the lungs of FVB mice (Fig. 4a). In the lungs of macIL-10^{tg} mice, however, gene expression was found to be even higher on days 49 and 90 post-infection. In contrast, 49 and 90 days after *Mtb* infection, gene expression of *IL-12p40* (*Il12b*) was found to be significantly reduced in lungs from macIL-10^{tg} mice when compared to FVB mice (Fig. 4b).

After *Mtb* infection, IL-12 is essential for driving protective TH1 immune responses (33). In lymphoid organs, IL-10 inhibits IL-12-driven TH1 development, whereas it has no suppressive effect on already differentiated TH1 cells in infected tissue (34). Because *Mtb*-infected macIL-10^{tg} mice displayed a normal TH1 development, we speculated that the magnitude of transgenic IL-10 expression would be different in draining lymph nodes and lung tissue. In contrast to dendritic cells, only few macrophages are present in lymph nodes in experimental TB (35). Accordingly, we found only low levels of IL-10 in lymph nodes from macIL-10^{tg} mice (Fig. 4c). In contrast, a great amount of IL-10 was secreted in lung tissue from

macIL-10^{tg} animals. In FVB mice, IL-10 was below detection limit in either organ (Fig. 4c). In line with the low expression of transgenic IL-10 in the lymph nodes of *Mtb*-infected macIL-10^{tg} mice, IL-12p40 expression was not affected. In contrast, elevated levels of transgenic IL-10 in lung tissue led to reduced expression of IL-12p40 (Fig. 4d). Taken together, IL-10 secretion by macrophages does not seem to have an overt effect on TH1 differentiation and the expression of TH1 cell effector mechanisms. Macrophage-derived IL-10 rather appears to regulate distinct macrophage functions such as cytokine secretion at the site of infection.

Impact of Mtb infection on pulmonary gene expression in wildtype and macIL-10^{tg} mice

To investigate how macrophage-specific overexpression of IL-10 shapes the host response to *Mtb* at the transcriptome level, genome-wide expression analysis was performed on tissue RNA isolated from the lungs of FVB and macIL-10^{tg} mice at baseline as well as 25 and 42 days after infection. Excluding variability for the infection itself, only 219 probe sets were different between FVB and macIL-10^{tg} , indicating a comparatively small effect of IL-10 on the transcriptional changes. The effect of IL-10 on the number of up- and down-regulated genes is summarized in Fig. 5a. Prior to infection, only 36 probesets were upregulated in lungs from macIL-10^{tg} mice compared to FVB animals (data not shown). These included some known IL-10-induced genes (*Msr1*, *Ccr2*, *Ccr5*, *Fcgr2b*, *Saa3*). Only four probesets, all detecting *Igg*, gave significantly higher signals in lungs from FVB mice. After infection, at the early time point d25, of all probesets induced more than threefold in either lung RNA from wildtype or macIL-10^{tg} mice, only one probeset (*C3ar1*) had significantly increased expression in macIL-10^{tg} mice, whereas *Igh-VJ588* was higher in FVB control animals. Of the 970 probe sets induced by *Mtb* 42 days after infection, 158 showed higher expression in macIL-10^{tg}, whereas 68 were significantly higher in lungs from wildtype mice. Therefore, the majority of IL-10 effects was apparent at the later stages of infection.

Hierarchical clustering of the probe sets regulated by IL-10 (Fig. 5b, data are listed in Supplementary Table 1) revealed groups of genes overexpressed in the lungs of macIL-10^{tg} mice already under basal conditions (cluster A) or post-infection (cluster B). These clusters contained known target genes of IL-10 in macrophages like *Socs3*, *Bcl3*, *Saa3* and *Il1rn*, consistent with previous observations (31). However, many chemokines (e.g. *Ccl2*, *Ccl7*) and cytokines (*Il1b*, *Il6*) were also expressed at higher levels in the lungs of macIL-10^{tg} mice compared to wildtype animals, indicating that the inhibitory effect of IL-10 on proinflammatory gene expression is likely affected by the increased bacterial load in macIL-10^{tg} mice.

Data mining: changes in cellular composition

The presence of various transcripts encoding cell type-specfic surface proteins, such as the dendritic cell marker *Cd207* in cluster C and the monocyte/macrophage marker *Msr1* in cluster B, suggested an impact of IL-10 on the infection-induced changes in the cellular composition of the lung tissue. We used a literature-based data mining tool, Genomatix Bibliosphere, to search for overrepresentation of anatomical terms in lists of genes upregulated in macIL-10^{tg} or wildtype mice after *Mtb* infection (Fig. 6a). While transcriptional evidence for NK cells, dendritic cells and T lymphocytes was similar in both genotypes, in the lungs of macIL-10^{tg} mice a strong enrichment for probe sets associated with macrophages was evident. In contrast, probe sets upregulated to higher levels in FVB lungs at d42 were connected to B lymphocytes. Immunohistological analysis also revealed a moderately reduced infiltration of B cells in lungs from macIL-10^{tg} mice (Supplementary Figure 1). Together, IL-10 appears to regulate leukocyte subset migration to the lung, or local proliferation of the cells, during *Mtb* infection.

Signs of alternative macrophage activation in the lung transcriptome after Mtb infection

Among the group of genes induced to high levels in infected macIL-10^{tg} mice was *Arg1 (Fig. 6b)*, encoding the enzyme arginase-1, whose extrahepatic expression is typically associated with IL-4/IL-13-induced alternative macrophage activation indicating that after *Mtb* infection IL-10 may promote the development of alternatively activated macrophages. While *Il4* and *Il13* mRNA was not detectably expressed in the lung dataset, small amounts of IL-4 or IL-13 could promote alternative activation of lung macrophages in macIL-10^{tg} mice. IL-10 may enhance the sensitivity to IL-4 because it increases IL-4 receptor-alpha (*Il4ra*) expression on macrophages *in vitro* (31), an effect that was also observed in the lung dataset after *Mtb* infection (Fig. 6b). In addition to arginase-1, many other markers have been described to define IL-4 receptor-alpha (Rα)-mediated alternatively activated macrophages especially during pulmonary inflammation such as Fizz1, various chitinases and the macrophage mannose receptor (MMR) (36). Among these genes, only *Fizz1* (encoded by *Retlna*) and the chitinase *Chi3l1* were clearly expressed at higher levels in macIL-10^{tg} lungs (Fig. 6b), whereas the chitinases *Ym1* (=*Chi3l3*) and *Ym2* (=*Chi3l4*) as well as the *Mmr* (encoded by *Mrc1*) were downregulated after infection to similar levels in both genotypes. The differential induction of markers for alternatively activated macrophages in *Mtb*-infected macIL-10^{tg} mice reflects also some opposite biological effects of IL-10 to IL-4 and IL-13 e.g. the regulation of MMR expression and function (37). In contrast to this rather inhibitory effect, IL-10 has been clearly shown to contribute to alternative macrophage activation during Toll-like receptor ligation by a strong synergistic induction of Arginase-1 (31). Together, our genome wide expression analysis revealed that after infection with *Mtb*, macrophage-derived IL-10 induces several features of alternatively activated macrophages.

After Mtb-infection, macIL-10^{tg} mice develop alternatively activated macrophages

To verify our findings revealed by genome-wide expression analysis, we next performed qRT-PCR analysis to test the model that macrophage-derived IL-10 promotes alternative macrophage activation after *Mtb* infection (Fig. 7a). Six weeks after infection, we found significantly elevated gene expression of *Fizz1* and *Arg1*. In contrast, transcripts for *Mmr* and the chitinase *Ym1* were not elevated. In whole tissue, *Il4ra* gene expression in macIL-10^{tg} mice was elevated but not significantly different from gene expression in lungs from FVB wildtype mice. To determine the activation state of macrophages in *Mtb*-infected macIL-10^{tg} mice, we analysed macrophages from perfused lungs by flow cytometry. Six weeks after infection IA^{q}, CD80, CD86, and the MMR were expressed to the same extent on PI-negative F4/80-positive cells from FVB and macIL-10^{tg} mice (Fig. 7b). Whereas only a subpopulation of macrophages from infected FVB mice expressed the IL-4Rα, all macrophages from macIL-10^{tg} mice were found to be positive for this receptor subunit. Together, we found that after *Mtb* infection IL-10 secretion by macrophages induces an alternatively activated program characterized by an enhanced expression of *Fizz1*, *Arg1* and the *Il4ra*.

In Mtb-infected macIL-10^{tg} mice, increased arginase-1 activity is concomitant with reduced production of RNI

Classical macrophage activation plays an important role in combating infection with *Mtb* through IFNγ-induced expression of effector molecules such as NOS2-dependent RNI (4). This induction may be counter-regulated in alternatively activated macrophages. Because in alternatively activated macrophages arginase-1 hydrolyses L-arginine to urea and L-ornithine this pathway is also discussed to regulate RNI production in macrophages through depletion of L-arginine as the substrate for NOS2 (38,39). Therefore, we speculated that in macIL-10^{tg} mice an increased arginase-1 activity modulates the production of RNI thereby affecting effector mechanisms against *Mtb* usually exerted by classically activated macrophages. A kinetic quantification of gene expression revealed that *Arg1* is not induced in lungs from FVB

mice during the course of *Mtb*-infection (Fig. 8a). In contrast, *Arg1* expression in macIL-10^{tg} mice was found to be significantly induced during the late phase of *Mtb* infection. Accordingly, arginase activity in lungs from macIL-10^{tg} mice was found to be elevated already 49 days post-infection (Fig. 8c). In contrast, arginase activity was detectable in the lungs of FVB mice but did not increase after infection (Fig. 8b). Concomitant with the increased arginase-1 activity in infected macIL-10^{tg} mice, RNI were only moderately produced in these animals (Fig. 8c). In distinction, significantly increasing amounts of RNI were found in sera from *Mtb*-infected FVB mice (Fig. 8c). Hence, the increased susceptibilty in macIL-10t^{g} mice after infection with *Mtb* appeared to be caused by an elevated induction of arginase-1 in alternatively activated macrophages which in turn led to an inefficient production of RNI. To examine whether IL-10-induced arginase-1 expression in macrophages diminishes anti-mycobacterial effector mechanisms in macrophages, we performed a *Mtb* growth inhibition assay in arginase-1-deficient BMMϕ (Fig. 8d). Incubation of BMMϕ from Tie2^{cre}-neg Arg-1$^{flox/flox}$ arginase-1-competent and Tie2^{cre}-pos Arg-1$^{flox/flox}$ arginase-1-deficient mice lead to a significant reduction of mycobacterial growth 48 and 72 h after infection with *Mtb* when compared to infected macrophages that have not been activated with IFNγ. Pre-incubation with IL-4 and IL-10, however, diminished IFNγ-dependent mycobacterial growth inhibition in arginase-1-competent BMMϕ. In contrast, IL-4/IL-10 treatment of IFNγ-activated arginase-1-deficient macrophages did not lead to reduced anti-mycobacterial effector mechanisms indicating that induction of arginase-1 in macrophages reduces the capability of controling *Mtb* growth.

macIL-10^{tg} mice control bacterial growth after M. avium infection

To test our hypothesis that macrophage-derived IL-10 mostly subverts NOS2-dependent effector mechanisms, we infected macIL-10^{tg} mice aerogenically with *M. avium*, a pathogen that is insensitive to NOS2-derived RNI production (6,40), and determined bacterial loads in different organs 105 days after infection (Fig. 9). Bacterial loads in macIL-10^{tg} mice were found to be only moderately increased in lung and liver, and comparable to FVB mice in spleens. However, infection of NOS2$^{-/-}$ mice with *M. avium* revealed that bacterial loads have been described to rather decreased in the absence of NOS2 (40) corroborating the contention that after infection with RNI-insensitive mycobacteria the suppressive effect of nitric oxide on T cells appears (6). Therefore, the inability of macIL-10^{tg} mice to efficiently control bacterial growth after infection with RNI-sensitive and to some extend also - insensitive mycobacteria indicates that autocrine IL-10 operates partially by reducing RNI production via arginase-1 induction.

DISCUSSION

TB is a systemic disease that becomes manifest most prominently in the lung (24). Progressive primary TB occurs when the initial inflammatory focus is unable to contain mycobacterial replication and the disease spreads to other parts of the lung. Post-primary disease develops when a lesion containing a previously “dormant”, i.e. growth-arrested, organism resumes growth after a period of clinical latency. This organism may have been implanted years before during a primary infection that was successfully contained by a protective TH1 type immune response. Reactivation is often a consequence of a perturbed immune status of the host, although the cause of deregulation may be multifactorial.

Elevated levels of the TH2 cytokine IL-10 were detected in individuals with active tuberculosis (18,19). Importantly, macrophages rather than T cells were reported to be the major source of IL-10 in these patients (18). However, whether and how macrophage-derived IL-10 promotes exacerbation of primary infection or reactivation of chronic, latent infection is not clear. Our study revealed that in macIL-10^{tg} mice an increased production of IL-10 by macrophages

resulted in enhanced *Mtb* replication particularly during the chronic phase of infection, and thus bears some resemblance to reactivation TB in humans.

Humans infected with *Mtb* typically have a strong DTH response, as measured by the PPD skin test (24). This holds also true for patients suffering from post-primary TB. Thus, despite an apparently adequate initial differentiation of cell-mediated immune responses, *Mtb* is capable of persisting and can even resume replication within macrophages. In the draining lymph nodes of *Mtb*-infected macIL-10^{tg} mice T cells efficiently differentiated into TH1 cells and migrated to the site of infection. In spite of the presence of macrophage-derived IL-10 in the lungs of infected transgenic mice, TH1 cells efficiently expressed effector functions and secreted sufficient IFNγ to induce a classical macrophage activation characterized by expression of NOS2 and LRG-47. However, bacteria survived and successfully proliferated within IFNγ-activated IL-10^{tg} macrophages. It appears, therefore, that during experimental TB macrophage-derived IL-10 does not affect initiation and maintenance of TH1 immune responses but specifically acts on macrophage functions in a partially dominant manner over IFNγ at the functional level.

It is important to note that overexpression of IL-10 specifically in T cells resulted in completely different immunosuppressive mechanisms after *Mtb* infection (22). tIL-10^{tg} mice failed to efficiently prime naïve CD4^{+} T cells in draining lymph nodes resulting in decreased numbers of activated T cells in the blood circulation and lung tissue; this defective TH1 response eventually led to an increased bacterial burden, due to a failure of classical macrophage activation. In contrast, IL-10 expression in macrophages at the site of infection induces an alternative activation program specifically in macrophages that counteracts concomitant classical macrophage activation. Since T cell-mediated immune responses remain largely unaffected (as is the case in human post-primary TB), the outcome of experimental TB in macIL-10^{tg} mice may therefore better reflect the situation in patients with reactivating TB.

We could link the increased susceptibility of *Mtb*-infected macIL-10^{tg} mice neither to an impaired function of IFNγ-producing T cells nor to defective IFNγ-dependent downstream mechanisms in macrophages. Transcriptome analysis revealed a strong enrichment for probe sets associated with macrophage function in the lungs of *Mtb*-infected macIL-10^{tg} mice. IL-10 has previously been shown to act primarily on activated macrophages, where IL-10 receptor (IL-10R) expression is highest. The IL-10R activates STAT3 and loss of this transcription factor in macrophages mimics loss of IL-10 itself (41). Hence, because STAT3 in myeloid cells is both necessary and sufficient for the effects of IL-10 macrophages are major targets of IL-10 *in vivo* (41-44). On a functional level, IL-10 has been shown to negatively regulate macrophage function in a variety of experimental systems (17,29,30,45). *In vitro*, IL-10 antagonizes the IFNγ-dependent induction of NOS2 (29,30). Our finding that macIL-10^{tg} mice fail to efficiently control bacterial growth especially after infection with RNI-sensitive mycobacteria corroborates our contention that the mode of action of autocrine IL-10 proceeds minly via arginase-1 mediated reduction of RNI production in macrophages. However, we found NOS2 normally expressed in *Mtb*-infected macIL-10^{tg} mice whereas the production of RNI was reduced during the course of infection. Hence, other pathways must be affected in macrophages of macIl-10^{tg} mice that lead to an impaired expression of effector molecules such as RNI.

Among the group of genes induced to high levels in *Mtb*-infected macIL-10^{tg} mice some were associated with alternative macrophage activation such as *Il4ra*, *Fizz1* and *Arg1*. (36). Alternative macrophage activation is typically induced by IL-4Rα ligation. While *Il4* and *Il13* mRNA was not detectably expressed in the lung dataset, small amounts of IL-4 may still drive alternative activation of lung macrophages in macIL-10^{tg} mice. IL-10 may enhance the sensitivity to IL-4 because it increases IL-4 receptor expression on macrophages *in vitro* (31),

an effect that was also observed in the lung dataset after *Mtb* infection. The differential induction of markers for alternatively activated macrophages in *Mtb*-infected macIL-10^{tg} mice reflects also some opposite biological effects of IL-10 to IL-4 and IL-13 e.g. the regulation of MMR expression and function (37). In contrast to this rather inhibitory effect, IL-10 has been clearly shown to contribute to alternative macrophage activation during Toll-like receptor ligation by a strong synergistic induction of Arginase-1 (31). Hence, during experimental TB *Arg1* expression may be directly induced by IL-10 or indirectly by IL-10-dependent upregulation of the high affinity IL-4Rα. Alternative activation of macrophages via the IL-4Rα has been shown to differentially regulate protective and immunopathological immune responses (36). Importantly, analysis of macrophage-specifc IL-4Rα-deficient mice clearly demonstrated immunomodulation by macrophages to be a central regulatory mechanism during inflammatory immune responses *in vivo* (46). Because alternative macrophage activation reduces RNI production (39,47,48) and pro-inflammatory cytokine release (49), protective (38,50,51) and pathological (49) immune responses are significantly regulated by this type of macrophages.

In the context of TB and alternatively activated macrophages one genome-wide expression analysis in IL-4 stimulated murine bone marrow-derived macrophages infected with Mtb has been published so far (50). A specific re-analysis of our lung transcriptome data for differences in the expression of the 15 most highly increased genes in *Mtb*-infected IL-4-stimulated macrophages revealed that 5 genes were expressed at significantly higher levels in macIL-10^{tg} lungs than in FVB mice after infection (*Fcrg2b*, *Fn1*, *Cish*, *Ccl9*, *Mrc1*) and *Cdh1* was increased under basal conditions in macIL-10^{tg} lungs (data not shown). *Mmp12* (encoding matrix metalloproteinase-12, MMP-12) and *Tfr* (encoding the transferrin receptor, TfR) were found to be significantly upregulated in *Mtb*-infected alternatively activated macrophages *in vitro* (50). The induction of the TfR appears to be of major importance in the context of experimental TB because intracellular *Mtb* exploit the transferrin-transferring receptor complex for iron utilization (52). However, neither our genome-wide expression analysis nor quantitative RT-PCR revealed a differential regulation of *Tfr* in *Mtb*-infected macIL-10^{tg} mice *in vivo* (data not shown). Additionally, Kahnert and colleagues suggested MMP-12 induced in alternatively activated macrophages to be involved in the pathogenesis of TB (50). Though our genome-wide expression analysis in *Mtb*-infected macIL-10^{tg} mice revealed an increased expression of *Mmp12* in macIL-10^{tg} mice at later time points of infection, the difference was not significant (data not shown). Moreover, quantitative RT-PCR of *Mmp12* did not confirm a difference between wildtype and macIL-10^{tg} mice (data not shown). Together, genome-wide expression analysis in *Mtb*-infected and IL-4-induced alternatively activated macrophages *in vitro* and in *Mtb*-infected macIL-10^{tg} mice *in vivo* revealed an overlapping set of regulated genes, consistent with our interpretation that IL-10 supports a macrophage phenotype *in vivo* that is phenotypically related to alternatively activated macrophages.

Until recently little was known about the impact of alternative macrophage activation and arginase-1 on the outcome of *Mtb* infection. Classical macrophage activation plays a central role in combating infection with *Mtb* through IFNγ-induced expression of effector molecules such as the NOS2-dependent production of RNI (4,53). Importantly, inhibition of endogenous NOS2 reactivates latent infection in *Mtb*-infected mice, indicating that NOS2-dependent mechanisms in macrophages are crucial for the control of *Mtb* persisting in immunocompetent hosts (54). The production of RNI might be counter-regulated by IL-4Rα- and/or IL-10-dependent mechanisms, leading to arginase-1 expressing alternatively activated macrophages. In fact, RNI production in *Mtb*-infected alternatively activated macrophages was found to be reduced (50). In line with these findings we here show the induction of arginase-1 in macrophages subverts IFNγ-induced anti-mycobacterial effector mechanisms in macrophages. Since NOS2 shares L-arginine as a substrate with arginase-1, substrate depletion by either

enzyme is a key regulatory mechanism in macrophages and differential expression of NOS2 and arginase-1 is important for regulating macrophage effector functions (39,48). Very recently, El Kasmi *et al.* showed that specific deletion of arginase-1 in macrophages reduced lung bacterial loads during *Mtb* infection supporting our contention that arginase-1 induction in macrophages undermines NOS2-dependent effector mechanisms against *Mtb* by depletion of the common substrate L-arginine (26). In addition, arginase-dependent production of polyamines were shown to promote elevated growth of *Leishmania major* in macrophages (51) and may also be beneficial for the proliferation of *Mtb*. Importantly, in human pulmonary TB, high production of IL-10 also parallels arginase activity in peripheral-blood mononuclear-cells (55). Hence, elevated IL-10-dependent arginase activity during the chronic phase of infection may promote recrudescence of *Mtb* growth. We do not exclude that macrophage-derived IL-10 suppresses other anti-mycobacterial effector mechanisms in addition to regulating RNI synthesis. In contrast to infection with *Mtb*, macIL-10^{tg} mice were indeed able to control bacterial growth after infection with *M. avium*, which has been shown to be insensitive to the effects of RNI (6,40). However, because bacterial loads have been described to be further reduced after infection with *M. avium* in the complete absence of RNI in NOS2$^{-/-}$ mice, it appears that although autocrine IL-10 subverts RNI synthesis in macrophages other suppressive mechanisms may also be induced by IL-10.

We conclude that during *Mtb* infection macrophage-derived IL-10 drives reactivation during the chronic stage of the disease by acting primarily at the level of the macrophage. Macrophage-derived IL-10 appears to override IFNγ-dependent classical macrophage activation and effector mechanisms against *Mtb* by inducing an alternatively activated phenotype. Specifically, *Arg1* expression in these macrophages may provide better growth conditions for *Mtb*. TH2 cytokines that potently drive alternative macrophage activation have been associated with the development of post-primary TB in patients (7,56). Thus, reactivating TB may, in part, be mediated by a TH2 type immune reaction characterized by an alternative activation state of macrophages that eventually subverts protective immune mechanisms. It is possible that the identification of an increased type 2 cytokine immune response may identify infected individuals at risk to reactivate a latent *Mtb* infection. Additionally, prophylactic treatment of these individuals with immunomodulating drugs aimed at inhibiting the production of type 2 cytokines or downstream immune mechanisms may prevent or ameliorate reactivation TB.

Supplementary Material

Refer to Web version on PubMed Central for supplementary material.

Acknowledgements

The authors thank Alexandra Hölscher, Tanja Sonntag, Susanne Metken and Manfred Richter for excellent technical assistance; Ilka Monath, Sven Mohr and Claus Möller for organising the animal facility and taking care of the mice at the Research Center Borstel; Angela Servatius for management of the macIL-10^{tg} colony and processing the microarray samples at the Institute of Medical Microbiology, Immunology and Hygiene, Technical University Munich; Bianca Schneider for help with the *Mtb* growth inhibition assay.

References

1. Kaufmann SH. Tuberculosis: back on the immunologists' agenda. Immunity 2006;24:351–357. [PubMed: 16618591]
2. Cooper AM, Dalton DK, Stewart TA, Griffin JP, Russell DG, Orme IM. Disseminated tuberculosis in interferon gamma gene-disrupted mice. J. Exp.Med 1993;178:2243–2247. [PubMed: 8245795]
3. Flynn JL, Goldstein MM, Chan J, Triebold KJ, Pfeffer K, Lowenstein CJ, Schreiber R, Mak TW, Bloom BR. Tumor necrosis factor-alpha is required in the protective immune response against *Mycobacterium tuberculosis* in mice. Immunity 1995;2:561–572. [PubMed: 7540941]

4. MacMicking JD, North RJ, LaCourse R, Mudgett JS, Shah SK, Nathan CF. Identification of nitric oxide synthase as a protective locus against tuberculosis. Proc. Natl. Acad. Sci. U.S.A 1997;94:5243–5248. [PubMed: 9144222]
5. MacMicking JD, Taylor GA, McKinney JD. Immune control of tuberculosis by IFN-gamma-inducible LRG-47. Science 2003;302:654–659. [PubMed: 14576437]
6. Ehlers S, Benini J, Held HD, Roeck C, Alber G, Uhlig S. αβ T Cell Receptor-positive Cells and Interferon-γ, but not Inducible Nitric Oxide Synthase, Are Critical for Granuloma Necrosis in a Mouse Model of Mycobacteria-induced Pulmonary Immunopathology. J .Exp. Med 2001;194:1847–1859. [PubMed: 11748285]
7. Rook GA. Th2 cytokines in susceptibility to tuberculosis. Curr. Mol. Med 2007;7:327–337. [PubMed: 17504117]
8. Moore KW, de Waal Malefyt R, Coffman RL, O'Garra A. Interleukin-10 and the interleukin-10 receptor. Annu. Rev. Immunol 2001;19:683–765. [PubMed: 11244051]
9. Lang R. Tuning of macrophage responses by STAT3-inducing cytokines: molecular mechanisms and consequences in infection. Immunobiology 2005;210:63–76. [PubMed: 16164013]
10. Murray PJ. Understanding and exploiting the endogenous interleukin-10/STAT3-mediated anti-inflammatory response. Curr. Opin. Pharmacol 2006;6:379–386. [PubMed: 16713356]
11. D'Andrea A, Aste-Amezaga M, Valiante NM, Ma X, Kubin M, Trinchieri G. Interleukin 10 (IL-10) inhibits human lymphocyte interferon gamma-production by suppressing natural killer cell stimulatory factor/IL-12 synthesis in accessory cells. J. Exp. Med 1993;178:1041–1048. [PubMed: 8102388]
12. Macatonia SE, Doherty TM, Knight SC, O'Garra A. Differential effect of IL-10 on dendritic cell-induced T cell proliferation and IFN-gamma production. J. Immunol 1993;150:3755–3765. [PubMed: 8097224]
13. Berg DJ, Kuhn R, Rajewsky K, Muller W, Menon S, Davidson N, Grunig G, Rennick D. Interleukin-10 is a central regulator of the response to LPS in murine models of endotoxic shock and the Shwartzman reaction but not endotoxin tolerance. J. Clin. Invest 1995;96:2339–2347. [PubMed: 7593621]
14. Kühn R, Lohler J, Rennick D, Rajewsky K, Müller W. Interleukin-10-deficient mice develop chronic enterocolitis. Cell 1993;75:263–274. [PubMed: 8402911]
15. Dai WJ, Köhler G, Brombacher F. Both innate and acquired immunity to *Listeria monocytogenes* infection are increased in IL-10-deficient mice. J. Immunol 1997;158:2259–2267. [PubMed: 9036973]
16. Kane MM, Mosser DM. The role of IL-10 in promoting disease progression in leishmaniasis. J. Immunol 2001;166:1141–1147. [PubMed: 11145695]
17. Hölscher C, Mohrs M, Dai WJ, Köhler G, Ryffel B, Schaub GA, Mossmann H, Brombacher F. Tumor necrosis factor alpha-mediated toxic shock in *Trypanosoma cruzi*-infected interleukin 10-deficient mice. Infect. Immun 2000;68:4075–4083. [PubMed: 10858224]
18. Barnes PF, Lu S, Abrams JS, Wang E, Yamamura M, Modlin RL. Cytokine production at the site of disease in human tuberculosis. Infect. Immun 1993;61:3482–3489. [PubMed: 8335379]
19. Verbon A, Juffermans N, Van Deventer SJ, Speelman P, Van Deutekom H, Van Der Poll T. Serum concentrations of cytokines in patients with active tuberculosis (TB) and after treatment. Clin. Exp. Immunol 1999;115:110–113. [PubMed: 9933428]
20. North RJ. Mice incapable of making IL-4 or IL-10 display normal resistance to infection with *Mycobacterium tuberculosis*. Clin. Exp. Immunol 1998;113:55–58. [PubMed: 9697983]
21. Murray PJ, Young RA. Increased antimycobacterial immunity in interleukin-10-deficient mice. Infect. Immun 1999;67:3087–3095. [PubMed: 10338525]
22. Turner J, Gonzalez-Juarrero M, Ellis DL, Basaraba RJ, Kipnis A, Orme IM, Cooper AM. In vivo IL-10 production reactivates chronic pulmonary tuberculosis in C57BL/6 mice. J. Immunol 2002;169:6343–6351. [PubMed: 12444141]
23. Murray PJ, Wang L, Onufryk C, Tepper RI, Young RA. T cell-derived IL-10 antagonizes macrophage function in mycobacterial infection. J. Immunol 1997;158:315–321. [PubMed: 8977205]
24. Ehlers, S.; Hölscher, C. DTH-associated pathology.. In: Kaufmann, SH., editor. Microbiology and microbial infections. Arnold Publsihing; London, U.K.: 2005. p. 705-720.

25. Lang R, Rutschman RL, Greaves DR, Murray PJ. Autocrine Deactivation of Macrophages in Transgenic Mice Constitutively Overexpressing IL-10 Under Control of the Human CD68 Promoter. J. Immunol 2002;168:3402–3411. [PubMed: 11907098]
26. El Kasmi KC, Qualls JE, Pesce JT, Smith AM, Thompson RW, Henao-Tamayo M, Basaraba RJ, König T, Schleicher U, Koo MS, Kaplan G, Fitzgerald KA, Tuomanen EI, Orme IM, Kanneganti TD, Bogdan C, Wynn TA, Murray PJ. Toll-like receptor-induced arginase 1 in macrophages thwarts effective immunity against intracellular pathogens. Nat. Immunol 2008;9:1399–1406. [PubMed: 18978793]
27. Hölscher C, Köhler G, Müller U, Mossmann H, Schaub GA, Brombacher F. Defective nitric oxide effector functions lead to extreme susceptibility of *Trypanosoma cruzi*-infected mice deficient in gamma interferon receptor or inducible nitric oxide synthase. Infect. Immun 1998;66:1208–1215. [PubMed: 9488415]
28. Benjamini Y, Hochberg Y. Controlling the false discovery rate: a practical and powerful approach to multiple testing. J. Roy. Stat. Soc 1995;57:289–300.
29. Flesch IE, Hess JH, Oswald IP, Kaufmann SH. Growth inhibition of *Mycobacterium bovis* by IFN-gamma stimulated macrophages: regulation by endogenous tumor necrosis factor-alpha and by IL-10. Int. Immunol 1994;6:693–700. [PubMed: 8080840]
30. Gazzinelli RT, Oswald IP, James SL, Sher A. IL-10 inhibits parasite killing and nitrogen oxide production by IFN-gamma-activated macrophages. J. Immunol 1992;148:1792–1796. [PubMed: 1541819]
31. Lang R, Patel D, Morris JJ, Rutschman RL, Murray PJ. Shaping Gene Expression in Activated and Resting Primary Macrophages by IL-10. J. Immunol 2002;169:2253–2263. [PubMed: 12193690]
32. Bogdan C, Paik J, Vodovotz Y, Nathan C. Contrasting mechanisms for suppression of macrophage cytokine release by transforming growth factor-beta and interleukin-10. J. Biol. Chem 1992;267:23301–23308. [PubMed: 1429677]
33. Cooper AM, Magram J, Ferrante J, Orme IM. Interleukin 12 (IL-12) is crucial to the development of protective immunity in mice intravenously infected with *Mycobacterium tuberculosis*. J. Exp. Med 1997;186:39–45. [PubMed: 9206995]
34. Fiorentino DF, Zlotnik A, Vieira P, Mosmann TR, Howard M, Moore KW, O'Garra A. IL-10 acts on the antigen-presenting cell to inhibit cytokine production by Th1 cells. J. Immunol 1991;146:3444–3451. [PubMed: 1827484]
35. Bhatt K, Hickman SP, Salgame P. Cutting edge: a new approach to modeling early lung immunity in murine tuberculosis. J. Immunol 2004;172:2748–2751. [PubMed: 14978073]
36. Gordon S. Alternative activation of macrophages. Nat. Rev. Immunol 2003;3:23–35. [PubMed: 12511873]
37. Montaner LJ, da Silva RP, Sun J, Sutterwala S, Hollinshead M, Vaux D, Gordon S. Type 1 and type 2 cytokine regulation of macrophage endocytosis: differential activation by IL-4/IL-13 as opposed to IFN-gamma or IL-10. J. Immunol 1999;162:4606–4613. [PubMed: 10202000]
38. Hölscher C, Arendse B, Schwegmann A, Myburgh E, Brombacher F. Impairment of Alternative Macrophage Activation Delays Cutaneous Leishmaniasis in Nonhealing BALB/c Mice. J. Immunol 2006;176:1115–1121. [PubMed: 16394000]
39. Rutschman R, Lang R, Hesse M, Ihle JN, Wynn TA, Murray PJ. Cutting edge: Stat6-dependent substrate depletion regulates nitric oxide production. J. Immunol 2001;166:2173–2177. [PubMed: 11160269]
40. Gomes MS, Florido M, Pais TF, Appelberg R. Improved clearance of *Mycobacterium avium* upon disruption of the inducible nitric oxide synthase gene. J. Immunol 1999;162:6734–6739. [PubMed: 10352292]
41. Takeda K, Clausen BE, Kaisho T, Tsujimura T, Terada N, Förster I, Akira S. Enhanced Th1 activity and development of chronic enterocolitis in mice devoid of Stat3 in macrophages and neutrophils. Immunity 1999;10:39–49. [PubMed: 10023769]
42. Williams LM, Ricchetti G, Sarma U, Smallie T, Foxwell BM. Interleukin-10 suppression of myeloid cell activation--a continuing puzzle. Immunology 2004;113:281–292. [PubMed: 15500614]

43. Williams L, Bradley L, Smith A, Foxwell B. Signal transducer and activator of transcription 3 is the dominant mediator of the anti-inflammatory effects of IL-10 in human macrophages. J. Immunol 2004;172:567–576. [PubMed: 14688368]
44. El Kasmi KC, Holst J, Coffre M, Mielke L, de Pauw A, Lhocine N, Smith AM, Rutschman R, Kaushal D, Shen Y, Suda T, Donnelly RP, Myers MG Jr. Alexander W, Vignali DA, Watowich SS, Ernst M, Hilton DJ, Murray PJ. General nature of the STAT3-activated anti-inflammatory response. J. Immunol 2006;177:7880–7888. [PubMed: 17114459]
45. Bogdan C, Vodovotz Y, Nathan C. Macrophage deactivation by interleukin 10. J. Exp. Med 1991;174:1549–1555. [PubMed: 1744584]
46. Herbert DR, Hölscher C, Mohrs M, Arendse B, Schwegmann A, Radwanska M, Leeto M, Kirsch R, Hall P, Mossmann H, Claussen B, Förster I, Brombacher F. Alternative macrophage activation is essential for survival during schistosomiasis and downmodulates T helper 1 responses and immunopathology. Immunity 2004;20:623–635. [PubMed: 15142530]
47. Hesse M, Modolell M, La Flamme AC, Schito M, Fuentes JM, Cheever AW, Pearce EJ, Wynn TA. Differential regulation of nitric oxide synthase-2 and arginase-1 by type 1/type 2 cytokines in vivo: granulomatous pathology is shaped by the pattern of L-arginine metabolism. J. Immunol 2001;167:6533–6544. [PubMed: 11714822]
48. Munder M, Eichmann K, Modolell M. Alternative metabolic states in murine macrophages reflected by the nitric oxide synthase/arginase balance: competitive regulation by $CD4^+$ T cells correlates with Th1/Th2 phenotype. J. Immunol 1998;160:5347–5354. [PubMed: 9605134]
49. Herbert DBR, Orekov T, Perkins C, Rothenberg ME, Finkelman FD. IL-4R α Expression by Bone Marrow-Derived Cells Is Necessary and Sufficient for Host Protection against Acute Schistosomiasis. J. Immunol 2008;180:4948–4955. [PubMed: 18354220]
50. Kahnert A, Seiler P, Stein M, Bandermann S, Hahnke K, Mollenkopf H, Kaufmann SH. Alternative activation deprives macrophages of a coordinated defense program to *Mycobacterium tuberculosis*. Eur. J. Immunol 2006;36:631–647. [PubMed: 16479545]
51. Kropf P, Fuentes JM, Fahnrich E, Arpa L, Herath S, Weber V, Soler G, Celada A, Modolell M, Müller I. Arginase and polyamine synthesis are key factors in the regulation of experimental leishmaniasis in vivo. FASEB J 2005;19:1000–1002. [PubMed: 15811879]
52. Schaible UE, Collins HL, Priem F, Kaufmann SH. Correction of the iron overload defect in beta-2-microglobulin knockout mice by lactoferrin abolishes their increased susceptibility to tuberculosis. J. Exp. Med 2002;196:1507–1513. [PubMed: 12461085]
53. Flesch IE, Kaufmann SH. Mechanisms involved in mycobacterial growth inhibition by gamma interferon-activated bone marrow macrophages: role of reactive nitrogen intermediates. Infect. Immun 1991;59:3213–3218. [PubMed: 1908829]
54. Chan J, Tanaka K, Carroll D, Flynn J, Bloom BR. Effects of nitric oxide synthase inhibitors on murine infection with *Mycobacterium tuberculosis*. Infect. Immun 1995;63:736–740. [PubMed: 7529749]
55. Zea AH, Culotta KS, Ali J, Mason C, Park HJ, Zabaleta J, Garcia LF, Ochoa AC. Decreased expression of CD3zeta and nuclear transcription factor kappa B in patients with pulmonary tuberculosis: potential mechanisms and reversibility with treatment. J. Infect. Dis 2006;194:1385–1393. [PubMed: 17054067]
56. Seah GT, Scott GM, Rook GA. Type 2 cytokine gene activation and its relationship to extent of disease in patients with tuberculosis. J. Infect. Dis 2000;181:385–389. [PubMed: 10608794]

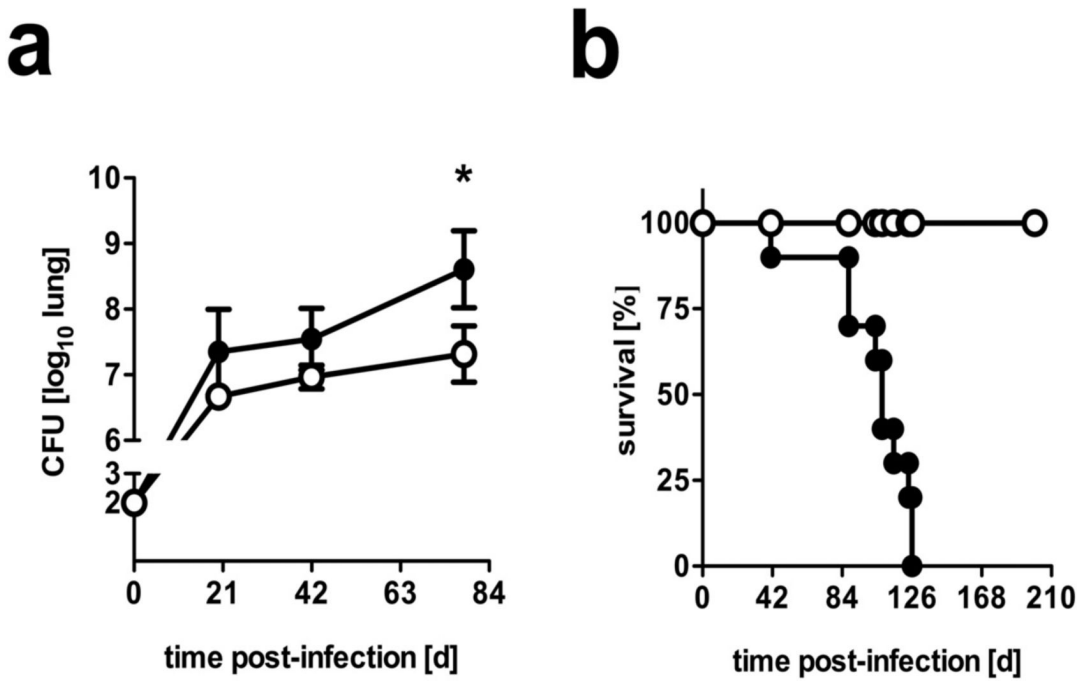

Figure 1. macIL-10^{tg} mice are highly susceptible to *Mtb* infection

FVB (open symbols) and macIL-10^{tg} (solid symbols) mice were infected with 100 CFU *Mtb* via the aerosol route. **(a)** For mycobacterial colony enumeration assays, lungs, were removed at the indicated time points and colony forming units were counted 21 days after plating of serial diluted organ homogenates. Data represent means and standard deviations of 4 mice. One experiment representative of three performed is shown. Statistical analysis was performed using the unpaired Student's *t* test defining differences between FVB and macIL-10^{tg} mice as significant (*, $p \leq 0.05$). **(b)** During the course of infection survival of 10 infected mice per group was monitored. Animals that lost more than 25% of their original body weight were sacrificed. Statistical analysis of the resulting survival curve was performed using the log rank test. Differences in survival kinetics between FVB and macIL-10^{tg} mice were highly significant ($p \leq 0.001$). Therefore, the experiment was terminated and remaining wild-type animals were euthanized in compliance with ethical guidelines for animal experimentation.

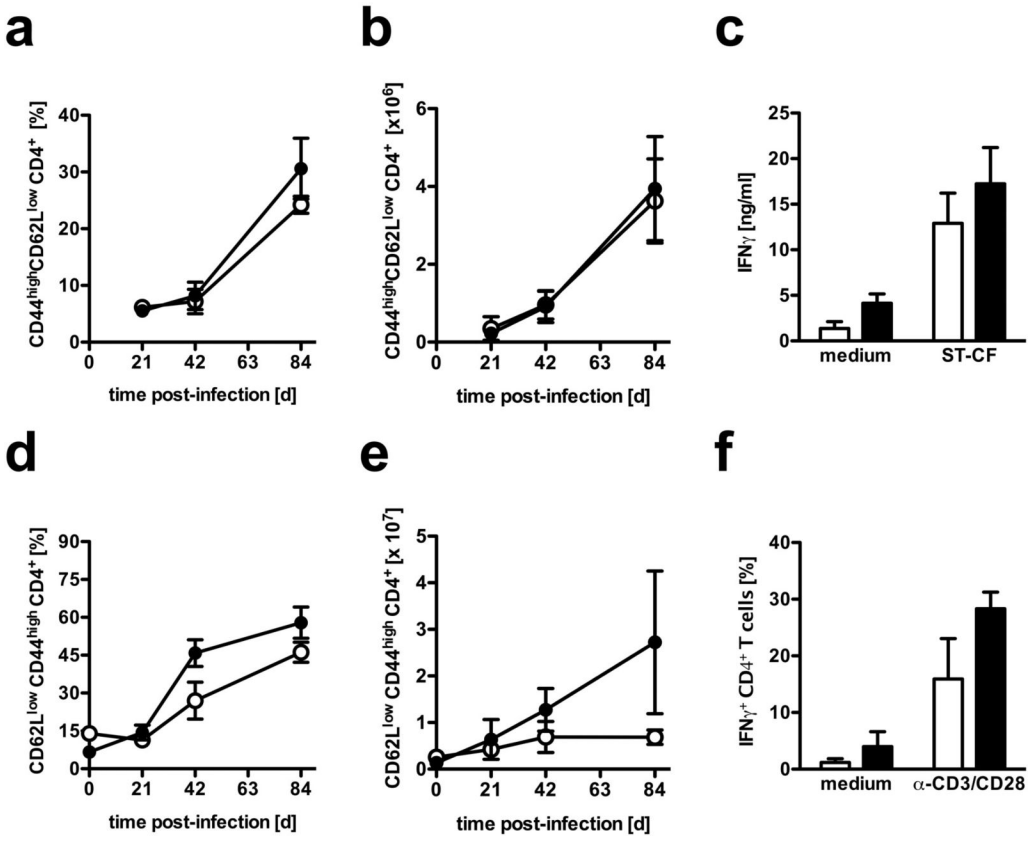

Figure 2. Normal recruitment and activation of T cells in macIL-10^{tg} mice after aerosol infection with *Mtb*

FVB (open symbols) and macIL-10^{tg} (solid symbols) mice were infected with 100 CFU *Mtb* via the aerosol route. At different time points, single cell suspensions from (a-c) draining lymph nodes and (e-f) lungs were prepared. Surface and activation markers were stained for flow cytometric analysis of activated **(a, b, d, e)** CD44^{high}CD62L^{low} CD4$^+$ T cells. The relative (a, d) and (b, e) absolute amount of activated CD4$^+$ T cells was calculated. Data represent means and standard deviations of 4 mice. One experiment representative of two performed is shown. **(c)** Antigen-specific restimulation of CD4$^+$ T cells from mediastinal lymph nodes was performed 21 days after infection. Enriched (>95%) CD4$^+$ T cells were cultivated in the presence of antigen-presenting peritoneal macrophages that have been pulsed with medium or ST-CF. After 72 h, the supernatants were assayed for IFNγ by ELISA. **(f)** Analysis of IFNγ production by CD4$^+$ T cells from lungs of infected mice was performed 21 days after infection. For detection of intracellular IFNγ, cells were stimulated with plate-bound anti-CD3/CD28 mAb for 4 h in the presence of GolgiPlug™. After staining for CD4, cells were fixed and permeabilized and intracellularly accumulated IFNγ was detected by a PE-labelled anti-IFNγ mAb. Data represent means of triplicate assays. Data represent means and standard deviations of 3 mice. One experiment representative of two performed is shown.

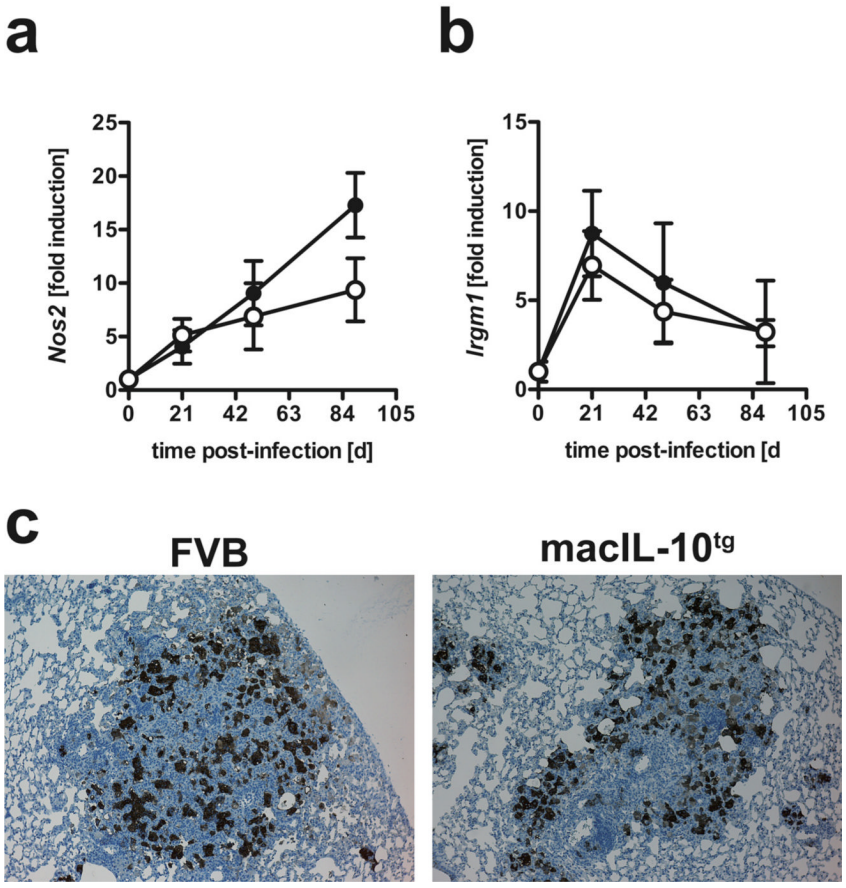

Figure 3. Efficient induction of IFNγ-dependent effector mechanisms in *Mtb*-infected macIL-10^{tg} mice

FVB (open symbols) and macIL-10^{tg} (solid symbols) mice were infected with 100 CFU *Mtb* via the aerosol route. Gene-expression of IFNγ-dependent **(a)** *Nos2* and **(b)** *LRG-47* (*lrgm1*) was determined in lung homogenates from uninfected and mice infected for 21, 49 and 89 days by RTPCR based on expression of *Hprt*. Data represent means and standard deviations of 3 mice. One experiment representative of two performed is shown. **(c)** For immunohistological detection of NOS2, 2−3 μm sections were prepared from FVB and macIL-10^{tg} mice 42 days after aerosol infection and staining was performed with a polyclonal rabbit anti-mouse NOS2 antibody. Representative results of 4 mice per group obtained in three independent experiments are shown.

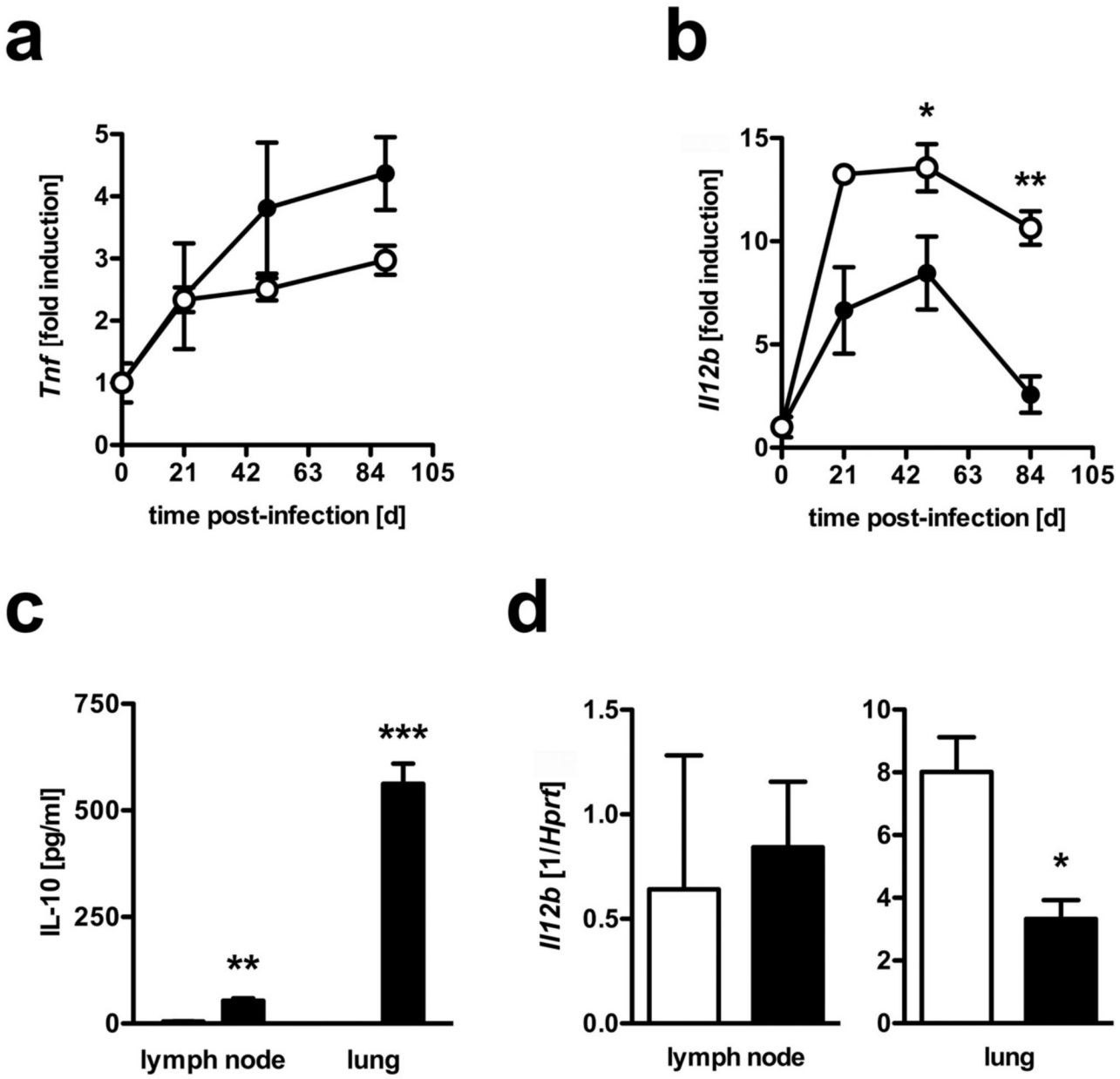

Figure 4. Differential production of IL-10 specifically suppresses IL-12p40 in infected tissue but not in draining lymph nodes

FVB (open symbols) and macIL-10^{tg} (solid symbols) mice were infected with 100 CFU *Mtb* via the aerosol route. Gene-expression of **(a)** *Tnf* and **(b)** *IL-12p40* (*Il12b*) was determined in lung homogenates from uninfected and mice infected for 21, 49 and 89 days by quantitative real time RT-PCR based on expression of *Hprt*. **(c)** After 42 days of infection, 3×10^6 cells from single cell suspensions of mediastinal lymph nodes and perfused lungs were cultured. After 24 h, the production of IL-10 was determined by ELISA. **(d)** Gene-expression of *IL-12p40* (*Il12b*) was determined in mediastinal lymph node and lung homogenates from mice infected for 42 days by RT-PCR based on expression of *hprt*. Data represent means and standard deviations of 3 mice. One experiment representative of two performed is shown. Statistical analysis was performed using the unpaired Student's *t* test defining differences between FVB and macIL-10^{tg} mice as significant (*, $p\leq0.05$; **, $p\leq0.01$***, $p\leq0.001$).

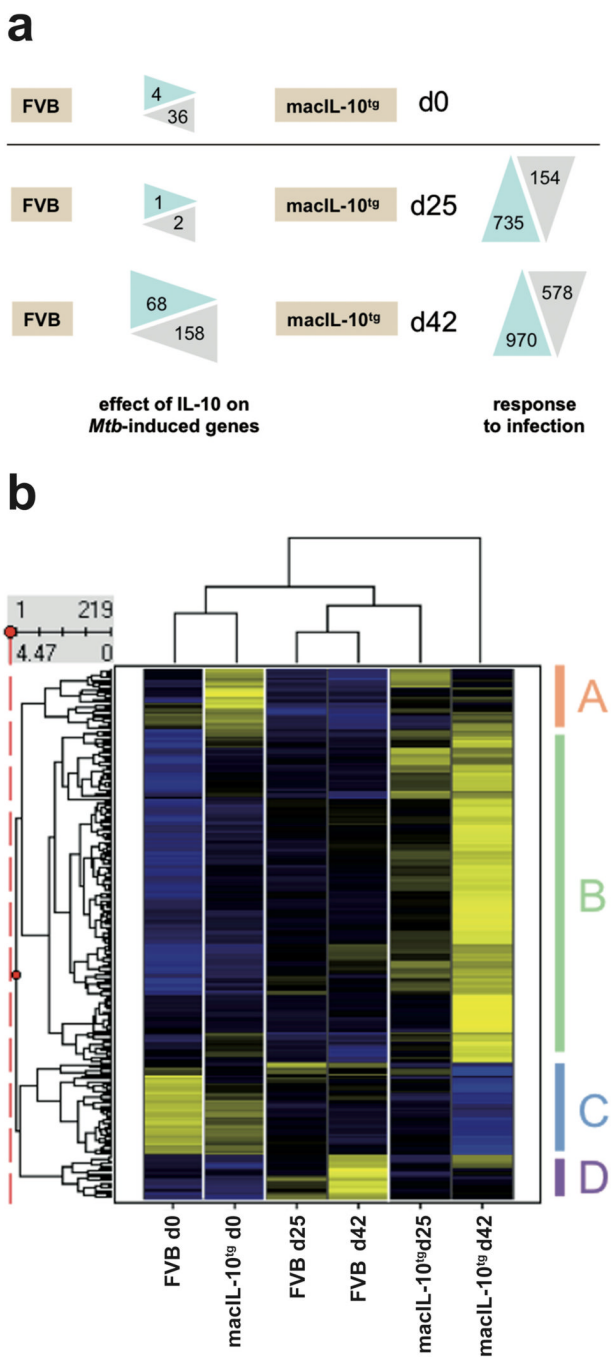

Figure 5. Pulmonary gene expression in wildtype and macIL-10^{tg} mice

FVB and macIL-10^{tg} mice were infected with 100 CFU *Mtb* via the aerosol route. Gene-expression analysis was performed in lung homogenates from uninfected and mice infected for 25 and 42 days. **(a)** Numbers of probe sets regulated by overexpression of IL-10 in *Mtb*-infected mice. After preselection of 4188 probe sets that were regulated across the experiment, for both time points the number of probe sets are shown that are up- or down-regulated more than three-fold in WT or macIL-10^{tg} mice ("response to infection"). Limma statistics was used to compare WT and macIL-10^{tg} mice. For d0, all 4188 preselected probe sets were used as the basis for comparison. At d25 and d42 after infection, the 735 and 970 genes up-regulated by infection were used to define statistically significant changes due to IL-10 overexpression.

(b) Hierarchical clustering of z-score normalized average expression values of 219 probe sets significantly different (Limma q value < 0.05) between FVB and macIL-10^{tg}. Yellow and blue colour indicates high and low relative expression, respectively.

a

Term	Association of genes (z-scores) highly expressed after *Mtb* infection	
	FVB	macIL-10^{tg}
Macrophages	1.3	**125.98**
Dendritic Cells	46.42	40.63
Natural Killer Cells	10.48	19.8
T-Lymphocytes	23.69	57.98
B-Lymphocytes	**112.02**	-3.75

b

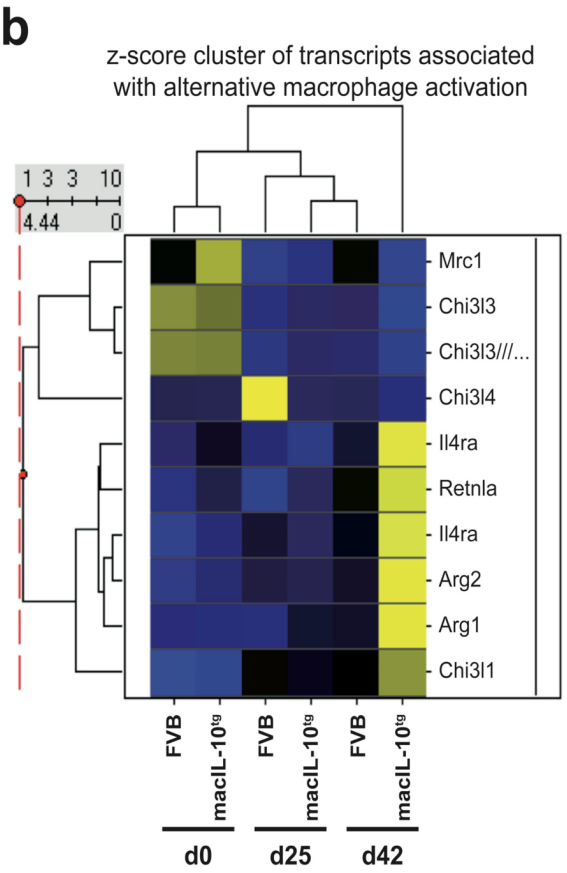

Figure 6. Signs of alternative macrophage activation in the lung transcriptome of macIL-10^{tg} mice after *Mtb* infection

(a) Gene lists identified in Fig. 5A as upregulated differentially in FVB and macIL-10^{tg} mice at d42 after infection were entered into the Genomatix Bibliosphere literature-based data mining tool. Shown are the z-score values indicating the degree of co-citation of selected cell types with the gene list from both genotypes. Higher z-score values indicate stronger enrichment. **(b)** Changes in expression of selected genes associated with alternative macrophage activation during *Mtb* infection of FVB and macIL-10^{tg} mice were visualized using hierarchical clustering of z-score normalized average expression values. Similarity

between experimental conditions and patterns of individual genes is indicated by dendrograms. Gene symbols are given.

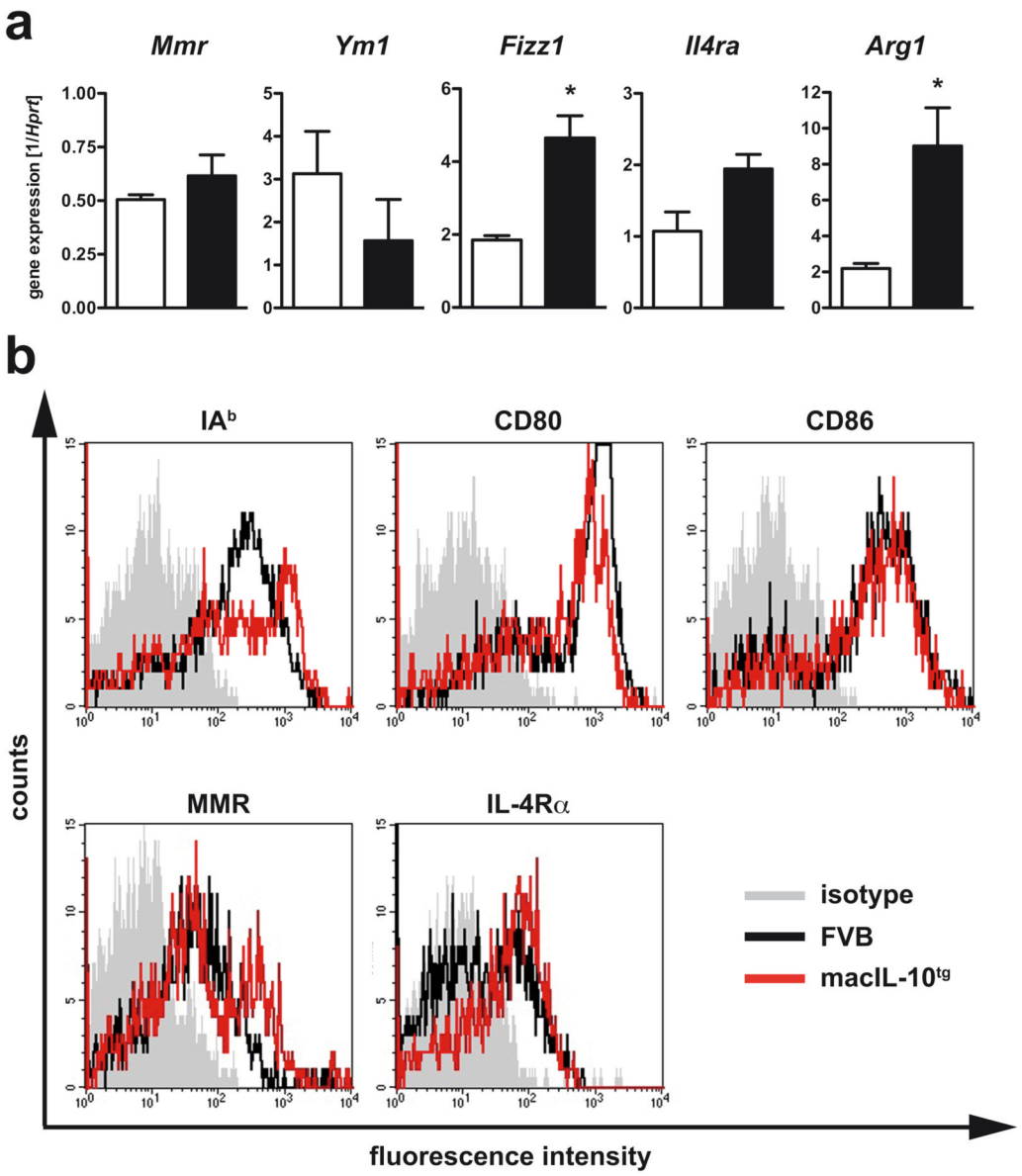

Figure 7. Enhanced alternative macrophage activation in lungs from *Mtb*-infected macIL-10^{tg} mice

FVB (open symbols) and macIL-10^{tg} (solid symbols) mice were infected with 100 CFU *Mtb* via the aerosol route. **(a)** Gene-expression of *Mmr*, *Ym1*, *Fizz1*, *Il4ra*, *Arg1* was determined in lung homogenates from mice infected for 42 days by quantitative real time RT-PCR based on expression of *hprt*. Statistical analysis was performed using the unpaired Student's *t* test defining differences between FVB and macIL-10^{tg} mice as significant (*, $p \leq 0.05$). **(b)** Expression of activation markers on pulmonary macrophages was assessed by flowcytometric analysis of IA^{q}, CD80, CD86, MMR, and IL-4Rα gated on PI^{-} F4/80^{+} cells in single cell suspensions of perfused lungs from FVB (black line) and macIL-10^{tg} mice (red line) mice. Representative histogram of 1 out of 3 mice per group (gray histogram, isotype control).

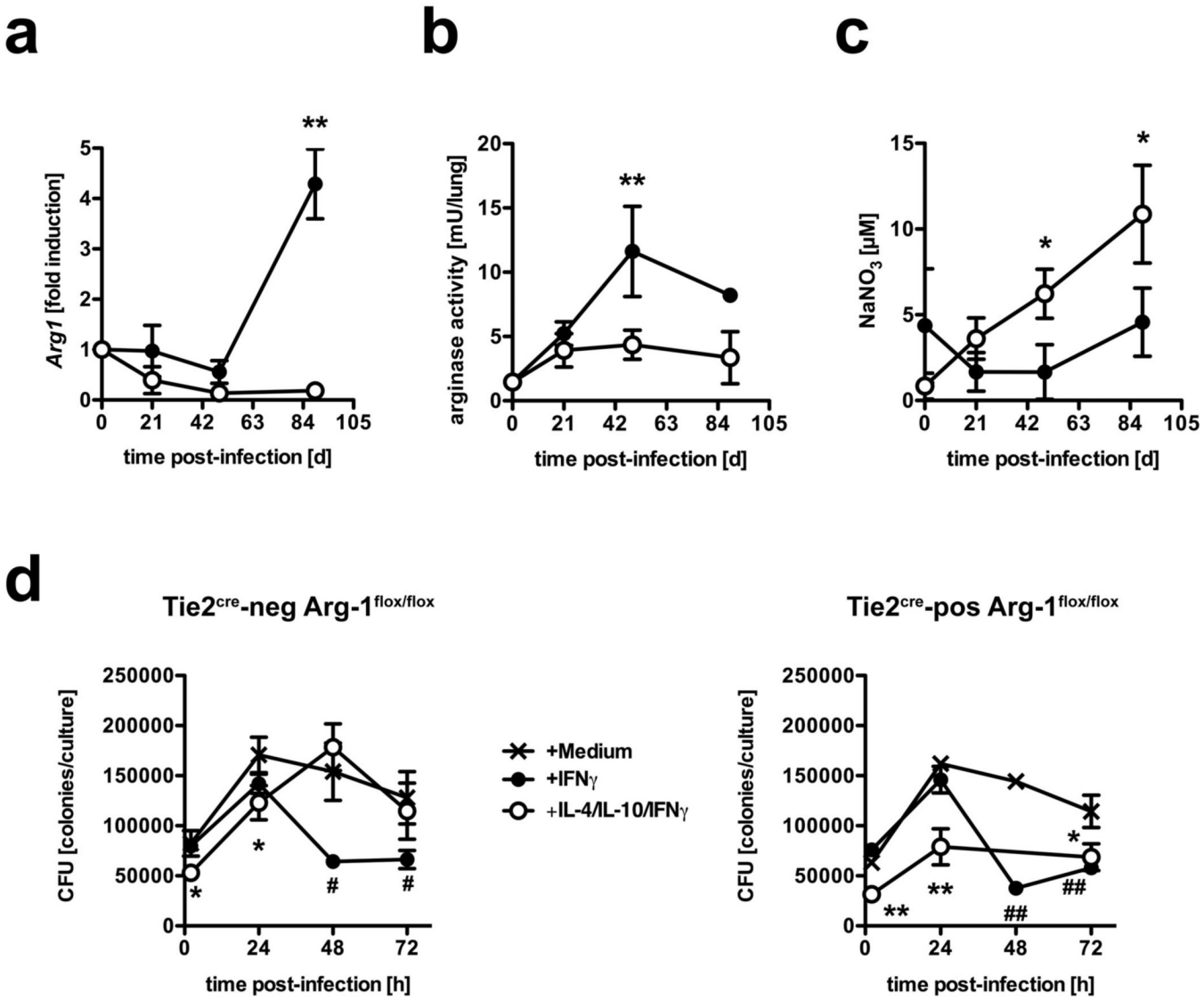

Figure 8. IL-10-dependent arginase-1 induction diminished anti-mycobacterial effector mechanisms

(a-c) FVB (open symbols) and macIL-10^{tg} (solid symbols) mice were infected with 100 CFU *Mtb* via the aerosol route. **(a)** Gene-expression of *Arg1* was determined in lung homogenates from uninfected and mice infected for 21, 49 and 89 days by quantitative real time RT-PCR based on expression of *hprt*. Data represent means and standard deviations of 3 mice. One experiment representative of three performed is shown. **(b)** At different time points, the degree of arginase activity in lungs from uninfected and infected mice was determined as urea production in homogenates of weighed pieces of lungs after addition of L-arginine. **(c)** During the course of infection, the RNI content in sera was measured by the Griess reaction. Statistical analysis in (a) - (c) was performed using the unpaired Student's *t* test defining differences between FVB and macIL-10^{tg} mice as significant (*, $p \leq 0.05$; **, $p \leq 0.01$). **(d)** BMMϕ were incubated with medium (crossed lines), IFNγ (solid symbols) or IL-4/IL-10/IFNγ (open symbols) and infected with *Mtb* at a MOI of 0.5. Colony forming units were counted 21 days after plating of serial diluted cell lysates. Data in (d) represent means and standard deviations of BMMϕ from 3 mice. ANOVA was performed using the Dunnett Multiple Comparison test), correcting for multiple testing, that defines different error probabilities between untreated cells

and macrophages that have been incubated with IFNγ (#, p≤0.05; ##, $p \leq 0.01$) or IL-4/IL-10/IFNγ (*, $p \leq 0.05$; **, $p \leq 0.01$.

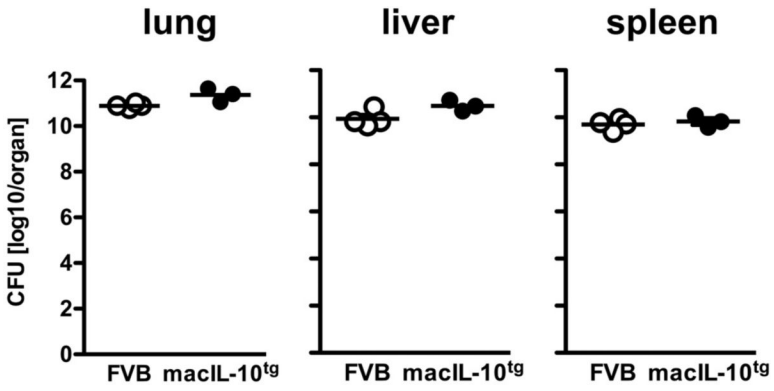

Figure 9. macIL-10^{tg} mice control bacterial growth after *M. avium* infection

FVB (open circles) and macIL-10^{tg} (solid circles) mice mice were infected with 10^5 CFU *M. avium* via the aerosol route. For mycobacterial colony enumeration assays, lungs, spleen and liver were removed 105 days after infection and colony forming units were counted 21 days after plating of serial diluted organ homogenates. Data represent means of 2 − 4 mice.